IL NUOVO CIMENTO **39 C** (2016) 300
DOI 10.1393/ncc/i2016-16300-4

Colloquia: SWGM 2015

Time-convolutionless mode-coupling theory near the glass transition: Numerical solutions for the Percus-Yevick model

Y. Kimura([1]) and M. Tokuyama([2])

([1]) *Department of Mechanical Engineering, Hachinohe National College of Technology Hachinohe 039-1192, Japan*
([2]) *Institute of Multidisciplinary Research for Advanced Materials, Tohoku University Sendai 980-8577, Japan*

received 19 July 2016

Summary. — The full numerical solutions of the time-convolutionless mode-coupling theory (TMCT) equation recently proposed by Tokuyama are compared with those of the ideal mode-coupling theory (MCT) equation based on the Percus-Yevick static structure factor for hard spheres qualitatively and quantitatively. The ergodic to non-ergodic transition at the critical volume fraction ϕ_c predicted by MCT is also shown to occur even for TMCT. Thus, ϕ_c of TMCT is shown to be much higher than that of MCT. The dynamics of coherent-intermediate scattering functions and their two-step relaxation process in a β stage are also discussed.

1. – Introduction

In 1984, the so-called ideal mode-coupling theory (MCT) has been proposed by Bengtzelius, Götze, and Sjölander [1], and independently by Leutheusser [2] to discuss the dynamics of supercooled liquids from first principles. Since then, the MCT equations for the intermediate scattering function $F_\alpha(q,t)$ have been numerically solved for various glass-forming systems [3-21], where $\alpha = c$ stands for collective case and $\alpha = s$ for self case. One of the most important predictions of MCT is an ergodic to non-ergodic transition at a critical temperature T_c (or a critical volume fraction ϕ_c). However, the numerical solutions have shown that T_c (or ϕ_c) is always much higher (or lower) than the thermodynamic glass transition temperature T_g (or ϕ_g), which is commonly defined by a crossover point seen in an enthalpy-temperature line [22]. Those numerical solutions are also shown to violate the original definition of the so-called non-Gaussian parameter $\alpha_2(t)$ at an initial time. In fact, MCT leads to $\alpha_2(t=0) = -2/3$ analytically, while the original definition requires to be 0. In order to overcome these problems, Tokuyama [23] has recently proposed the time-convolutionless mode-coupling (TMCT) equations for $F_\alpha(q,t)$ by employing exactly the same formulation as that used in MCT,

except that the time-convolutionless type projection operator method [24] is applied to derive a Langevin equation for the density, instead of the convolution type [25]. Then, in the previous paper [26] it has been suggested within a simplified model proposed by MCT that the critical temperature T_c is much lower than that of MCT. By applying the same mathematical formulation as that discussed by Götze [27,28] directly to the TMCT equation, it has been also shown that there exists a two-step relaxation process in a β stage near the critical point, which is described by exactly the same two different power-law decays as those obtained in MCT. Very recently, as a preliminary test of TMCT, we have also solved the TMCT equations numerically [29] based on the Percus-Yevick (PY) static structure factor for hard spheres [30] under exactly the same conditions as those employed in the previous calculations of the MCT equations [9]. Thus, we have shown that ϕ_c is much higher than that of MCT. In the present paper, therefore, we compare the TMCT solutions obtained for the PY model with those of MCT qualitatively and quantitatively.

2. – Basic equations

We consider the three-dimensional equilibrium glass-forming system, which consists of N particles with mass m and diameter σ_d in the total volume V at temperature T. We define the intermediate scattering function by $F_\alpha(q,t) = \langle \rho_\alpha(\boldsymbol{q},t)\rho_\alpha(\boldsymbol{q},0)^*\rangle$ with the collective density fluctuation $\rho_c(\boldsymbol{q},t) = N^{-1/2}[\sum_{j=1}^{N}\rho_s(\boldsymbol{q},t) - N\delta_{\boldsymbol{q},0}]$ and the self-density fluctuation $\rho_s(\boldsymbol{q},t) = e^{i\boldsymbol{q}\cdot\boldsymbol{X}_j(t)}$, where $\boldsymbol{X}_j(t)$ denotes the position vector of the j-th particle at time t and $q = |\boldsymbol{q}|$. Since the density fluctuations $\rho_\alpha(\boldsymbol{q},t)$ are macroscopic physical quantities, we set $q \le q_c$, where the inverse cutoff q_c^{-1} is longer than a linear range of the intermolecular force but shorter than a semi-macroscopic length and is in general fixed so that the numerical solutions coincide with the simulation results at least in a liquid state. Here $F_c(q,0) = S_c(q) = S(q)$ and $F_s(q,0) = S_s(q) = 1$, where $S(q)$ is a static structure factor.

As shown in the previous papers refs. [23,26], use of the time-convolutionless projection operator method [24] leads to the TMCT equation for $F_\alpha(q,t)$ given by

$$\frac{\partial F_\alpha(q,t)}{\partial t} = -q^2\int_0^t \psi_\alpha(\boldsymbol{q},\tau)\mathrm{d}\tau F_\alpha(q,t), \tag{1}$$

where the memory function $\psi_\alpha(\boldsymbol{q},t)$ is described by

$$\frac{\partial \psi_\alpha(\boldsymbol{q},t)}{\partial t} = -\gamma_\alpha\psi_\alpha(\boldsymbol{q},t) - \int_0^t \Delta\varphi_\alpha(\boldsymbol{q},t-\tau)\psi_\alpha(\boldsymbol{q},\tau)\mathrm{d}\tau, \tag{2}$$

γ_α being a positive constant. Here we note that the memory term of eq. (1) is convolutionless in time because $F_\alpha(q,t)$ describes a diffusion process, while that of eq. (2) is convolution in time because the current-current correlation function $\psi_\alpha(\boldsymbol{q},t)$ describes a mechanical process. The nonlinear memory function $\Delta\varphi_\alpha(\boldsymbol{q},t)$ is given by

$$\Delta\varphi_\alpha(\boldsymbol{q},t) = \frac{v_{\mathrm{th}}^2\rho}{2^{n_\alpha}}\int_< \frac{\mathrm{d}\boldsymbol{k}}{(2\pi)^3} v_\alpha(\boldsymbol{q},\boldsymbol{k})^2 F_c(k,t)F_\alpha(|\boldsymbol{q}-\boldsymbol{k}|,t), \tag{3}$$

where $\int_<$ denotes the sum over wave vectors $\boldsymbol{k}$ whose magnitudes are smaller than a cutoff q_c. Here $n_c = 1$, $n_s = 0$, $\rho = N/V$, and $v_{\mathrm{th}} = (k_BT/m)^{1/2}$. The vertex amplitude

$v_\alpha(\boldsymbol{q},\boldsymbol{k})$ is given by

$$v_\alpha(\boldsymbol{q},\boldsymbol{k}) = \hat{\boldsymbol{q}}\cdot\boldsymbol{k}c(k) + n_\alpha\hat{\boldsymbol{q}}\cdot(\boldsymbol{q}-\boldsymbol{k})c(|\boldsymbol{q}-\boldsymbol{k}|), \tag{4}$$

where $\rho c(k) = 1-1/S(k)$ and $\hat{\boldsymbol{q}} = \boldsymbol{q}/q$. Here we note that the nonlinear memory function given by eq. (3) has exactly the same form as that obtained in the ideal MCT within the MCT approximation.

Equation (1) is easily solved to obtain a formal solution

$$f_\alpha(q,t) = \frac{F_\alpha(q,t)}{S_\alpha(q)} = \exp[-K_\alpha(q,t)], \tag{5}$$

with the cumulant function [31]

$$K_\alpha(q,t) = q^2\int_0^t (t-\tau)\psi_\alpha(\boldsymbol{q},\tau)\mathrm{d}\tau. \tag{6}$$

As shown in the previous paper [26], use of eqs. (2) and (6) then leads to

$$\frac{\partial^2 K_\alpha(q,t)}{\partial t^2} = \frac{q^2 v_{\mathrm{th}}^2}{S_\alpha(q)} - \gamma_\alpha\frac{\partial K_\alpha(q,t)}{\partial t} - \int_0^t \Delta\varphi_\alpha(\boldsymbol{q},t-\tau)\frac{\partial K_\alpha(q,\tau)}{\partial\tau}\mathrm{d}\tau, \tag{7}$$

where the initial conditions for K_α are given by $K_\alpha(q,t=0) = \mathrm{d}K_\alpha(q,t)/\mathrm{d}t|_{t=0} = 0$. Equation (7) is an ideal TMCT equation to be compared with the ideal MCT equation discussed below.

The ideal MCT equation for the scaled scattering function $f_\alpha(q,t)$ is given by [1]

$$\frac{\partial^2 f_\alpha(q,t)}{\partial t^2} = -\frac{q^2 v_{\mathrm{th}}^2}{S_\alpha(q)}f_\alpha(q,t) - \gamma_\alpha\frac{\partial f_\alpha(q,t)}{\partial t} - \int_0^t \Delta\varphi_\alpha(\boldsymbol{q},t-\tau)\frac{\partial f_\alpha(q,\tau)}{\partial\tau}\mathrm{d}\tau. \tag{8}$$

Here we note that eqs. (7) and (8) have the same form, except for the first term. Applying the time-convolution projection operator method [25] to the starting equation for the density, one can also derive a new equation for $f_\alpha(q,t)$

$$\frac{\partial f_\alpha(q,t)}{\partial t} = -q^2\int_0^t \psi'_\alpha(\boldsymbol{q},t-\tau)f_\alpha(q,\tau)\mathrm{d}\tau, \tag{9}$$

where $\psi'_\alpha(\boldsymbol{q},t)$ is a memory function. As discussed in ref. [23], the memory function $\psi'_\alpha(\boldsymbol{q},t)$ is shown to be identical to $\psi_\alpha(\boldsymbol{q},t)$ within the MCT approximation. From eqs. (2) and (9), one can then derive eq. (8). Thus, eq. (9) is an equation to be compared with eq. (1). Next, we show that the difference between those starting equations in both theories causes significantly different results.

One of most important predictions of MCT is an existence of the ergodic to non-ergodic transition at a critical point, above which the scaled scattering function $f_\alpha(q,t)$ reduces to a non-zero value for long times, the so-called non-ergodicity parameter $f_\alpha(q)$. From eq. (8), one can find [1]

$$f_\alpha(q) = \lim_{t\to\infty}\frac{F_\alpha(q,t)}{S_\alpha(q)} = \frac{\mathcal{F}_\alpha(q)}{1+\mathcal{F}_\alpha(q)}, \tag{10}$$

with the long-time limit of the memory function

$$\mathcal{F}_\alpha(q, f_c, f_\alpha) = \frac{1}{2^{n_\alpha}(2\pi)^3} \int_< \mathrm{d}\boldsymbol{k} V_\alpha^{(2)}(q, k, |\boldsymbol{q}-\boldsymbol{k}|) f_c(k) f_\alpha(|\boldsymbol{q}-\boldsymbol{k}|), \tag{11}$$

where the vertex $V_\alpha^{(2)}$ is given by

$$V_\alpha^{(2)}(q, k, |\boldsymbol{q}-\boldsymbol{k}|) = \rho S_\alpha(q) S_c(k) S_\alpha(|\boldsymbol{q}-\boldsymbol{k}|) v_\alpha(\boldsymbol{q}, \boldsymbol{k})^2/q^2. \tag{12}$$

As shown in the previous papers [23, 26], this prediction also holds for TMCT. In fact, from eqs. (5) and (7) the non-zero solution is given by

$$f_\alpha(q) = \exp\left[-\frac{1}{\mathcal{F}_\alpha(q)}\right]. \tag{13}$$

Introducing the long-time cumulant function $K_\alpha(q)$ by $f_\alpha(q) = \exp[-K_\alpha(q)]$ and using eq. (13), one then finds

$$K_\alpha(q)\mathcal{F}_\alpha(q) = 1. \tag{14}$$

Equation (13) is a TMCT equation to find $f_\alpha(q)$ and is compared with the MCT equation given by eq. (10).

In order to estimate how the critical point obtained by eq. (14) is different from that by eq. (10), it is convenient to employ the simplified model discussed by Bengtzelius *et al.* [1]. Then, one can write $S(q)$ as $S(q) = 1 + A\delta(q - q_m)$, where A is a positive constant to be determined and q_m a wave vector of the first peak of $S(q)$. In the following, we only discuss the collective case for simplicity. Then, one can write eq. (11) as $\mathcal{F}_c(q_m) = \kappa f_c(q_m)^2$, where the coupling parameter κ is given by $\kappa = \rho q_m A^2 S(q_m)/(8\pi^2)$. Use of eqs. (10) and (11) then leads to a physically reasonable solution for MCT

$$f_c = 1/2 + (1/4 - 1/\kappa)^{1/2}. \tag{15}$$

From eq. (15), one can find the critical coupling parameter $\kappa_c = 4$ and the critical Debye-Waller factor $f_c^c = 1/2$. On the other hand, use of eqs. (11) and (14) leads to

$$\kappa K_c = e^{2K_c}. \tag{16}$$

This is the so-called Lambert W-function and has a physically reasonable solution for TMCT whose critical point is given by $\kappa_c = 2e(\simeq 5.43656)$, $K_c^c = 1/2$, and $f_c^c = e^{-K_c^c} = e^{-1/2}(\simeq 0.60653)$ [26]. Thus, the critical coupling parameter κ_c of TMCT turns out to be larger than that of MCT. In fact, as shown in the previous paper [26], this suggests that the critical temperature T_c (or the critical volume fraction ϕ_c) of TMCT is much lower (or higher) than that of MCT. This is confirmed later by solving the TMCT equations numerically based on the PY static structure factor.

The second important prediction of MCT is that there exists a two-step relaxation process in a β stage. As demonstrated in refs. [26, 27], one can directly apply exactly the same formulation as that employed by MCT to eq. (13) near ϕ_c. Thus, $f_c(q, t)$ is shown to obey exactly the same characteristic two-step relaxation process as that obtained by

MCT [28] at the so-called β-relaxation stage [β] near the critical point; the so-called critical decay at a fast β stage

$$f_c(q,t) = f_c^c(q) + h_q|\sigma|^{1/2}(t_\sigma/t)^a, \qquad t_0 \ll t \le t_\sigma, \tag{17}$$

and the so-called von Schweidler decay at a slow β stage

$$f_c(q,t) = f_c^c(q) - h_q(t/t'_\sigma)^b, \qquad t_\sigma \le t \ll t'_\sigma, \tag{18}$$

where f_c^c is a critical Debye-Waller factor, h_q a positive constant, and t_0 a microscopic time, $t_\sigma = t_0|\sigma|^{-1/2a}$, and $t'_\sigma = t_0 B^{-1/b}|\sigma|^\gamma$. Here $\gamma = 1/2a + 1/2b$ and B is a positive constant to be determined. The time exponents a and b are determined through the relation $\Gamma[1-a]^2/\Gamma[1-2a] = \Gamma[1+b]^2/\Gamma[1+2b] = \lambda$, where $\Gamma[x]$ is a gamma function of x. For the details of parameters, the reader is referred to ref. [28]. For the PY model, $\lambda(q_c)$ is calculated for MCT as $\lambda = 0.735$ at $q_c\sigma_d = 40$, leading to $a = 0.312$, $b = 0.583$, and $\gamma = 2.46$ [6]. Here we should note that in order to check whether the value of λ is the same as that of MCT or not, one must calculate it numerically under the same conditions as those employed in MCT. In the present paper, however, we just check instead whether the value obtained in MCT for the PY model is valid for TMCT or not. Finally, we mention that as shown in the previous paper ref. [32] the scattering function is also described by the logarithmic decay in a β stage as

$$f_c(q,t) = f_c^c - A\ln(t/t_\gamma) - B(t/t_\gamma)^C, \tag{19}$$

where A, B, and C are positive constant to be determined, and t_γ a characteristic time of β stage.

3. – Numerical solutions

We now solve the TMCT equations numerically by using the PY static structure factor under the same conditions as those employed by Chong *et al.* [9] to solve the MCT equations at $q_c\sigma_d = 40$ and $\gamma_\alpha = 0$. Here the MCT equations are also solved and the solutions are compared with the previous results obtained from refs. [9, 14] to check whether the present calculations are correct or not. The control parameter is the volume fraction given by $\phi = \pi\rho\sigma_d^3/6$. Following the former calculations by MCT, we also put $\gamma_\alpha = 0$. Although most of the MCT calculations have been done at $q_c\sigma_d = 40$, we here take three different cutoffs as $q_c\sigma_d = 10$, 20, and 40 for comparison. Thus, we compare the numerical solutions of TMCT with those of MCT.

We first discuss the critical volume fraction ϕ_c and the so-called Debye-Waller factor $f_c(q)$ for TMCT by solving eq. (14) with eq. (11) and also for MCT by solving eq. (10) with eq. (11). By changing the variables in the memory function $\mathcal{F}_c(q, f_c, f_c)$ given by eq. (11), one can easily write $\mathcal{F}_c(q, f_c, f_c)$ as

$$\mathcal{F}_c(q, f_c, f_c; q_c) = \frac{\rho S(q)}{32\pi^2 q^5} H(q, f_c, f_c; q_c), \tag{20}$$

TABLE I. – *Critical volume fraction ϕ_c for MCT and TMCT and a first peak position q_m of $f_c^c(q)$ at different wave vector cutoff q_c.*

Theory	ϕ_c		
	$q_c\sigma_d$ =10	20	40
MCT	0.5924	0.5214	0.5159
$(q_m\sigma_d)$	(7.398)	(7.093)	(7.070)
TMCT	0.695	0.5856	0.5817
$(q_m\sigma_d)$	(7.860)	(7.368)	(7.350)

with

$$H(q,f_c,f_c;q_c)=\int_0^{q_c}\mathrm{d}x\int_{|q-x|}^{|q+x|}\mathrm{d}yxyS(x)S(y)f_c(x)f_c(y)\times\left[(q^2+x^2-y^2)c(x)+(q^2-x^2+y^2)c(y)\right]^2. \tag{21}$$

Use of eq. (14) then leads for TMCT to

$$K_c(q)=\frac{32\pi^2q^5}{\rho S(q)H(q,f_c,f_c;q_c)}, \tag{22}$$

where $f_c(q)=\exp[-K_c(q)]$. On the other hand, use of eq. (10) leads for MCT to

$$f_c(q)=\frac{\rho S(q)H(q,f_c,f_c;q_c)}{32\pi^2q^5+\rho S(q)H(q,f_c,f_c;q_c)}. \tag{23}$$

Equations (22) and (23) are self-consistent equations to find the Debye-Waller factor $f_c(q)$ at a given value of q_c.

The values of ϕ_c and q_m are listed in table I. The critical point ϕ_c explicitly depends on the value of q_c, where ϕ_c increases as q_c decreases. Irrespectively of the value of q_c, ϕ_c of TMCT is always much higher than that of MCT. In fig. 1, the critical Debye-Waller factor $f_c^c(q)$ is plotted *versus* $q\sigma_d$ for different cutoffs $q_c\sigma_d=20$ and 40. Thus, it is shown that $f_c^c(q)$ of TMCT is larger than that of MCT since ϕ_c of TMCT is much higher than that of MCT. However, we should mention here that at volume fractions higher than ϕ_c of TMCT, the Debye-Waller factor $f_c(q)$ of MCT is always larger than that of TMCT. In order to check the present MCT numerical solutions, the previous MCT numerical solutions obtained for the PY static structure factor at $q_c\sigma_d=40$ by Voigtmann *et al.* [14] are also shown. Thus, the present MCT results are shown to agree with them within error.

We next discuss the numerical results obtained by solving the TMCT equation given by eq. (7) at $q_c\sigma_d=40$ and compare them with those of MCT. In figs. 2(A), the scaled coherent-intermediate scattering function $f_c(q,t)$ is plotted *versus* scaled time $v_{\mathrm{th}}t/\sigma_d$ for different volume fractions at $q_c\sigma_d=40$, where $q=q_m$. Here we note that although we neglect the numerical solutions of TMCT for $\phi\geq\phi_c$ in fig. 2(A), they also become constant to be $f_c(q)$. We should also mention here that even for smaller volume fractions the numerical results of TMCT do not agree with those of MCT, irrespectively of the

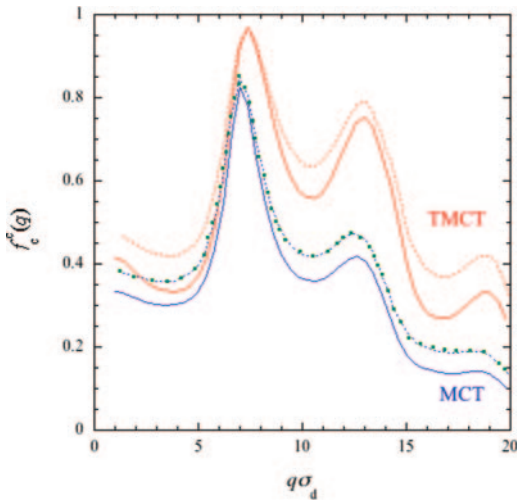

Fig. 1. – (Color online) A plot of the critical Debye-Waller factor $f_c^c(q)$ *versus* q. The solid lines indicate the numerical results for $f_c^c(q)$ at $q_c\sigma_d = 20$ and the dotted lines at $q_c\sigma_d = 40$ from ref. [29]. The symbols (•) indicate the numerical results at $q_c\sigma_d = 40$ from ref. [14].

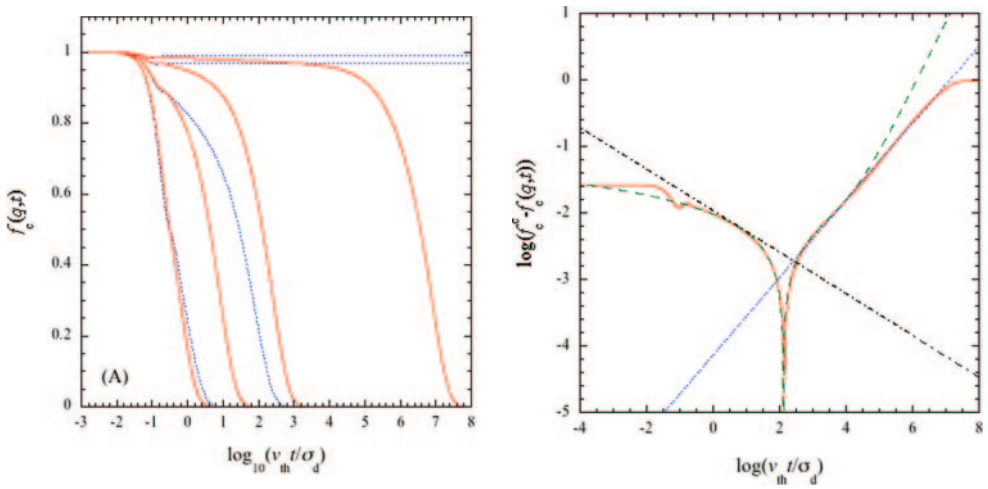

Fig. 2. – (Color online) (A) A plot of $f_c(q,t)$ *versus* scaled time $v_{\rm th}t/\sigma_d$ for different volume fractions at $q_c\sigma_d = 40$, where $q = q_m$. The solid lines indicate the TMCT results and the dotted lines the MCT results for ϕ =0.40, 0.50, 0.55, and 0.58 from left to right. (B) A log-log plot of $|f_c^c - f_c(q,t)|$ *versus* scaled time $v_{\rm th}t/\sigma_d$ for $\phi = 0.58$ at $q_c\sigma_d = 40$. The solid line indicates the TMCT results, the dot-dashed line the critical decay, the dotted line the von Schweidler decay, and the long-dashed line the logarithmic decay, where $\lambda = 0.735$ ($a = 0.312$ and $b = 0.583$), $f_c^c = 0.973$, $A = 1.9302 \times 10^{-3}$, $B = 1.0255 \times 10^{-4}$, $C = 1.0$, and $t_\gamma = 10^2.144\sigma_d/v_{\rm th}$.

value of q_c. For the PY model, λ is calculated at $q_c\sigma_d = 40$ for MCT as $\lambda = 0.735$, leading to $a = 0.312$, $b = 0.583$, and $\gamma = 2.46$ [6]. We now check whether this value also holds for TMCT results or not. In fig. 2(B), a log-log plot of $|f_c^c - f_c(q,t)|$ *versus* time is shown for $\phi = 0.58$ at $q_c\sigma_d = 40$, where $q = q_m$. Although the volume fraction 0.58 is not very close to the critical point ϕ_c, where $1 - \phi/\phi_c = 2.29 \times 10^{-3}$, the TMCT results can be described by the von Schweidler decay well, while they are also partially described by the critical decay. Thus, the value of λ calculated at $q_c\sigma_d = 40$ for MCT might be valid even for TMCT. Finally, we should mention here that the logarithmic decay can describe the numerical results in a fast β stage much better than the critical decay.

4. – Summary

In this paper, we have analyzed the numerical solution of the TMCT equations obtained by using the PY static structure factor under the same conditions as employed in the previous works for MCT and then compared their solutions with those of the MCT equations. We have shown that the critical volume fraction ϕ_c of TMCT is much higher than that of MCT, irrespectively of the magnitude of q_c (see table I). Then, we have compared the wave vector dependence of critical Debye-Waller factors of TMCT with that of MCT. We have also shown that there exists the same two-step relaxation process in a β stage as that discussed in MCT near ϕ_c. Very recently, this asymptotic behavior was also confirmed by Götze *et al.* [27]. In order to check whether TMCT can describe the dynamics of supercooled liquids reasonably well or not, the TMCT equations must be solved numerically by using the static structure factor obtained from the simulations and the experiments. This will be discussed elsewhere.

* * *

This work was partially supported by IMRAM, Tohoku University, Japan.

REFERENCES

[1] Bengtzelius U., Götze W. and Sjölander A., *J. Phys. C*, **17** (1984) 5915.
[2] Leutheusser E., *Phys. Rev. A*, **29** (1984) 2765.
[3] Fuchs M., Götze W., Hofacker I. and Latz A., *J. Phys.: Condens. Matter*, **3** (1991) 5047.
[4] Fuchs M., Hofacker I. and Latz A., *Phys. Rev. A*, **45** (1992) 898.
[5] Fuchs M., *Transp. Theory Stat. Phys.*, **24** (1995) 855.
[6] Franosch T., Fuchs M., Götze W., Mayr M. R. and Singh A. P., *Phys. Rev. E*, **55** (1997) 7153.
[7] Nauroth M. and Kob W., *Phys. Rev. E*, **55** (1997) 657.
[8] Winkler A., Latz A., Schilling R. and Theis C., *Phys. Rev. E*, **62** (2000) 8004.
[9] Chong S.-H., Götze W. and Mayr M. R., *Phys. Rev. E*, **64** (2001) 011503.
[10] Voigtmann Th., *Phys. Rev. E*, **68** (2003) 051401.
[11] Götze W. and Voigtmann Th., *Phys. Rev. E*, **29** (2003) 021502.
[12] Szamel G., *Phys. Rev. Lett.*, **90** (2003) 228301.
[13] Foffi G., Götze W., Sciortino F., Tartaglia P. and Voigtmann Th., *Phys. Rev. E*, **69** (2004) 011505.
[14] Voigtmann Th., Puertas A. M. and Fuchs M., *Phys. Rev. E*, **70** (2004) 061506.
[15] Flenner E. and Szamel G., *Phys. Rev. E*, **72** (2005) 031508.
[16] Voigtmann Th. and Horbach J., *Europhys. Lett.*, **74** (2006) 459.
[17] Tokuyama M. and Kimura Y., *Physica A*, **387** (2008) 4749.

[18] Götze W., *Complex Dynamics of Glass Forming Liquids: A Mode Coupling Theory* (Oxford Science, Oxford) 2009.
[19] Weysser F., Puertas A. M., Fuchs M. and Voigtmann Th., *Phys. Rev. E*, **82** (2010) 011504.
[20] Narumi T. and Tokuyama M., *Phys. Rev. E*, **84** (2011) 022501.
[21] Domschke M., Marsilius M., Blochowicz T. and Voigtmann Th., *Phys. Rev. E*, **84** (2011) 031506.
[22] Debenedetti P. G. and Stillinger F. H., *Nature*, **410** (2001) 259.
[23] Tokuyama M., *Physica A*, **395** (2014) 31.
[24] Tokuyama M. and Mori H., *Prog. Theor. Phys.*, **54** (1975) 918; **55** (1976) 411.
[25] Mori H., *Prog. Theor. Phys.*, **33** (1965) 423.
[26] Tokuyama M., *Physica A*, **430** (2015) 156.
[27] Götze W. and Schilling R., *Phys. Rev. E*, **91** (2015) 042117.
[28] Götze W., *Liquids, Freezing and Glass Transition*, edited by Hansen J. P., Levesque D. and Zinn-Justen J. (North-Holland, Amsterdam) 1991.
[29] Kimura Y. and Tokuyama M., arXiv:1407.3921 [cond-mat.stat-mech] (2014).
[30] Percus J. K. and Yevick G. J., *Phys. Rev.*, **110** (1958) 1.
[31] Kubo R., *J. Phys. Soc. Jpn.*, **17** (1962) 1100.
[32] Tokuyama M., *Physica A*, **364** (2006) 23.